ISSN 0001-4338, Izvestiya, Atmospheric and Oceanic Physics, 2020, Vol. 56, No. 12, pp. 1546–1559. © Pleiades Publishing, Ltd., 2020.
Russian Text © The Author(s), 2020, published in Issledovanie Zemli iz Kosmosa, 2020, No. 1, pp. 3–19.

USING SPACE-BASED INFORMATION ABOUT THE EARTH
GEOLOGICAL STUDIES FROM SPACE

Using Lineament Analysis to Identify Patterns in the Localization of Au Mineralization in the Taryn Gold Field in the Republic of Sakha (Yakutia)

D. V. Sivkov[a, b, *], A. F. Chitalin[a, b], and A. L. Dergachev[a]

[a] *Moscow State University, Moscow, 119991 Russia*
[b] *Institute of Geotechnology LLC, Moscow, 119234 Russia*
**e-mail: sivkovdmitrij@yandex.ru*

Received May 29, 2019; revised September 5, 2019; accepted October 28, 2019

Abstract—The development of geographic information systems and their growing application in Geology provide a unique opportunity to optimize the process of lineaments identification on images of the Earth's surface using the resources of laptops. The selection of primary linear objects is based on their searching in images in the form of linear and relatively extended boundaries between contrasting areas and/or sequences of pixels of the same tone. Such an analysis is performed for a large gold field in Eastern Sakha (Yakutia) territory to identify regional and local lineaments. Generally accepted models proposed to explain the orientation of faults in a homogeneous medium are used to interpret the results. Lineaments are found in the Taryn gold field that probably correspond to tectonic faults from three stages of compression. The assumed mutual position of the axes of the main normal stresses at different stages of deformation is confirmed by results from lineament analysis, interpreting the fracturing of an outcrop in the Bolshoi Taryn river valley, and exploratory drilling data.

Keywords: lineaments, geographic information systems, remote sensing, gold deposits, search features
DOI: 10.1134/S0001433820120543

INTRODUCTION

The term lineament was coined by the American geologist W. Hobbs (1904): "The more important lineaments of the earth physiognomy may be described as crests of ridges or the boundaries of elevated areas, the drainage lines, coastlines, and boundary lines of geologic formations, of petrographic rock types, or lines of outcrops." Lineament analysis is an effective complex of geomorphological, geological, remote sensing and other methods of mapping geological and geomorphological linear objects. Linear structures revealed as a result of research can be used to solve a number of applied problems. These include determining the paths of groundwater migration, searching for mineral deposits, and assessing the stability of geological blocks (Bondur and Zverev, 2005a, 2005b, 2007).

Tectonic faults in a rock mass and other geological objects (e.g., as fold axes) can often result in the formation of relatively straight morphological lines in the relief. Linear objects identified on satellite images, aerial photographs and digital terrain models, including straight-line outlines of valleys, slopes or ridges, can therefore represent a natural geological objects. Allocation of lineaments is usually done visually, along relatively straight segments of hydrographic and gully-girder networks, coastal lines of natural reservoirs, and microrelief forms. Analysis of vast territories (tens of km^2) in this way requires much time and great concentration.

With the development of geographic information systems and their increased use in geology, it became possible to optimize the process of identifying of lineaments using the resources of laptop computers. At the same time, the accuracy of identifying lineaments for both ways depends directly on the image resolution: high resolution allows us to distinguish short lineaments that are poorly expressed in relief.

GENERAL GEOLOGICAL INFORMATION

The Taryn gold field (TGF), which measures 16 × 17 km, is located in the East of the Republic of Sakha (Yakutia) in the Oymyakonsky district, 70 km south of the settlement Ust-Nera, the administrative center of the district. In structural and tectonic terms, this territory belongs to the Verkhne–Indigirka mega-synclinorium of the Yana–Indigirka synclinal zone in the structure of the Verkhoyansk–Kolyma folding system and is associated with Late Triassic flysch formations (Fig. 1).

In the late 1970s, a number of researchers (Vladimirov, 1977; Berger, 1978; Indolev et al., 1980) identified a connection between the Adycha–Taryn gold–antimony metallogenic zone with a hidden near vertical, deep-seated fault of the northwestern strike along

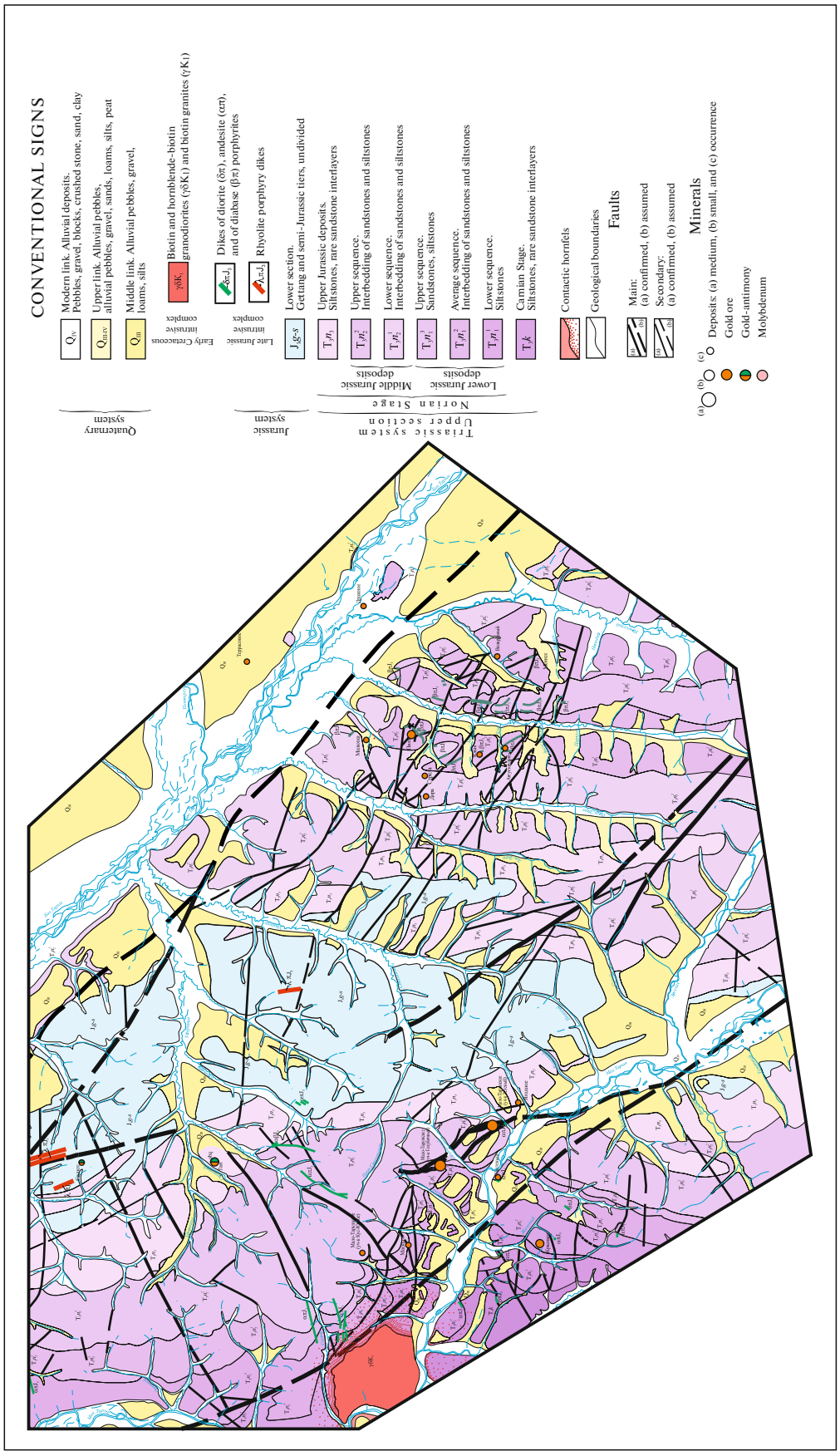

Fig. 1. Geological map of the Taryn gold field.

whose periphery areas of increased dislocation and fracturing of the host rocks were noted. The confinement of the largest and richest gold–quartz veins to the nodes of intersection of the main fracture with transverse faults was noted.

The TGF lies within the junction of the Taryn megasyncline and the Nel'kan brachyanticlinorium and is governed by the Bolshe–Taryn branch of the regional Adycha–Taryn deep fault (ATG), which extends for more than 1000 km (Mokshantsev et al., 1975). The role of the ore-governing structures is played by tectonic faults of the northwestern strike cutting across the northern part of the submeridional Pil anticline. Of no small importance within the area are the zones of northeastern and sublatitudinal strikes transverse to folding. These are usually high-angled faults with a displacement amplitude of up to the first tens of meters.

According to a number of studies, the Adycha-Taryn deep fault is a large left-lateral disjunctive zone (Parfenov L. M., 1988). The role of strike slip faults in the Yano–Kolyma region and Eastern Yakutia in the control of gold mineralization has been described in a number of works (Prokop'ev et al., 2000; Shahtyrov, 2009; Aristov et al., 2015; Voitenko, 2015; Chitalin, 2017; Chitalin et al., 2018). The authors also assumed the reversible nature of ATG kinematics (i.e., the occurrence of right-lateral after left-lateral movements).

The localization of mineralization is mainly determined by deformation that increases the permeability of the medium for ore-bearing solutions. With several phases of deformation, the degree of structural heterogeneity of the medium increases, producing sections of compression and decompression. Most of the gold deposits and signs of gold in the TGF are localized mainly in structures that are transverse to the ATG (in areas of tectonic faults, and in areas of increased fracturing of rocks). As shown by the results from analyzing different geological maps of the TGF, transverse faults to a greater extent have strike–slip (rather than fault) kinematics (Chitalin et al., 2018).

All vein–veinlet ore deposits known in the region are confined to local shear zones or faults of the WNW strike that cut the wings and hinge part of the regional Pil anticline at almost right angles. Ore bodies are represented by flat thick stockworks with disseminated veinlet quartz-sulfide mineralization with high gold content. The most permeable areas of steeply dipping tectonic faults act as ore-supplying and (less often) ore-hosting structures. Different structural models for the formation of gold-bearing stockworks have been proposed for the Drazhnoe gold deposit: a model of a combination of folded ore-controlling structures of interlayer delamination, thrust and shear (Aristov et al., 2015; Voitenko, 2015), and a model of a post-folded ore-controlling sinistral shear (Chitalin et al., 2018).

At one large TGF deposits, vein-disseminated gold–quartz mineralization is found only in stockworks of linear morphology and confined mainly to the core of the Pil anticline, which is composed of rocks enriched in carbonaceous (organic) matter and containing sulfide mineralization.

ANALYSIS OF TEXTURAL CHARACTERISTICS

Our analysis used an image obtained by the Landsat-8 OLI & TIRS system (September 13, 2017, at 01:51:14 and coordinates 143°00′04.8″ E and 63°48′49.4″ N (lower left corner) and 143°39′01.8″ E and 64°02′16.3″ N (upper right corner). The most of the work was done with the GIS ESRI ArcGIS (United States), PCI Geomatica Focus (Canada) and LESSA (Russia) software.

We analyzed textural characteristics to reveal how the locally predominant directions are distributed over parts of the territory that are homogeneous in terms of orientational properties, where anomalous zones and lines appear, and so on.

The technology used for lineament analysis, LESSA (Lineament Extraction and Stripe Statistical Analysis), allows us to analyze in a unified manner the orientation characteristics in raster images and DEM (Zlatopol'skiy, 2008). Orientation characteristics are measured in LESSA by identifying linear elements (stripes); i.e., the straightened borders of halftone areas in the image and ridges/valleys in the DEM, and the direction of the stripe is determined at each point. In a moving average, rose diagrams are calculated that reflect the distribution of stripes in the direction, and many derived characteristics also calculated. The results from the automated selection of linear objects within the Taryn ore field are shown in Fig. 2. A total of 24971 rectilinear objects with an average length of 355 m were identified. A specific density map of lineaments was calculated on basis of these objects' positions (Fig. 2). The map clearly shows an area of lower density, framed along the periphery by an area with a higher specific density of linear objects. The drop in the number of lineaments in this area is presumably associated with the presence at depth of an undiscovered deep intrusion, identified according to geophysical data, which is discussed below.

For further analysis, each segment of the lineaments was defined as the true azimuth of its strike ($0° \le$ str. az.$< 180°$). Based on this attribute, eight maps of relative lineament densities were constructed with azimuths $22.5° \pm 11.25°$, $45° \pm 11.25°$, $67.5° \pm 11.25°$, $90° \pm 11.25°$, $112.5° \pm 11.25°$, $135° \pm 11.25°$, $157.5° \pm 11.25°$ and $180° \pm 11.25°$ (Fig. 9). The maxima of the relative density of lineaments, which are arranged in linear chains and form some trends, are highlighted on all of our maps. As a rule, such trends are formed by many close co-directional lineaments. Linear maxima (trends) of density coinciding with lineaments in azimuth thus mark large linear geological objects. In Fig. 9, a linear trend of density maxima is clearly visible in the northeastern part of the studied ore field, in the form of strikes from northwest to

southeast in the valley of the Bolshoi Taryn river. This trend corresponds to a large regional fault zone, the Adycha–Taryn. A similar trend of the submeridional strike is found in the southwestern part of the site, the valley of the Maly Taryn river.

To improve detail and exclude the identification of man-made objects (roads, heating mains, power lines), the nature of each lineament in the areas of thickening was determined by superimposing it on a panchromatic satellite image. In many cases, large lineaments correspond to the valleys of small watercourses. It is assumed that in such cases, rivers and streams follow tectonic disturbances coming to the surface in areas of decompaction rocks. Some lineaments are easily traced across watersheds, often standing out in the shade in such areas.

Lineaments identified in this way were divided into three morphological groups, based on their size: small, medium, and large. Figure 9 clearly shows that the Taryn gold field is located between two large lineaments of the NW-SE strike. As noted above, large lineaments in the Bolshoi Taryn river valley correspond to the Adycha–Taryn fault zone. A large lineament in the Maly Taryn river valley (in the lower left corner of the Taryn ore field) also presumably follows a tectonic fault zone. The central part of the ore field is dominated by medium-sized lineaments of a submeridional and northeastern strike. Some of these correspond to the valleys of the Pil, Malyutka, Dora, and other streams. Such medium-sized lineaments are normally limited to large lineaments in the valleys of the Bolshoi and Maly Taryn rivers. Short lineaments within the ore field have predominantly sublatitudinal and NW–SE orientation and are limited to medium-sized lineaments. It is noteworthy that the lineaments are oriented in the NW–SE direction in the central and eastern parts of the ore field, and in the valley of the Bolshoi Taryn river.

FRACTURING IN THE BOLSHOI TARYN RIVER VALLEY

A photograph taken by A. F. Chitalin of the mesostructural forms in an outcrop in the Bolshoi Taryn river valley was used to confirm our results. The photograph was processed for further use in a graphic editor using basic algorithms to increase contrast, and to avoid interpretation errors (e.g., shadows cast by bushes as linear objects). The photo was further processed using the same algorithm as for satellite images, allowing us to identify a variety of differently oriented linear objects. For all linear items, a manual filter was used to remove misinterpreted areas where tree branches were located on the outcrop, or a hammer has been placed to visually determine the scale. The true strike azimuth was determined for each segment of the polylines. Statistics were later calculated for the entire set of segments with certain azimuths. The length of each segment was considered when calculating statistics (i.e., calculating rose diagrams). In other

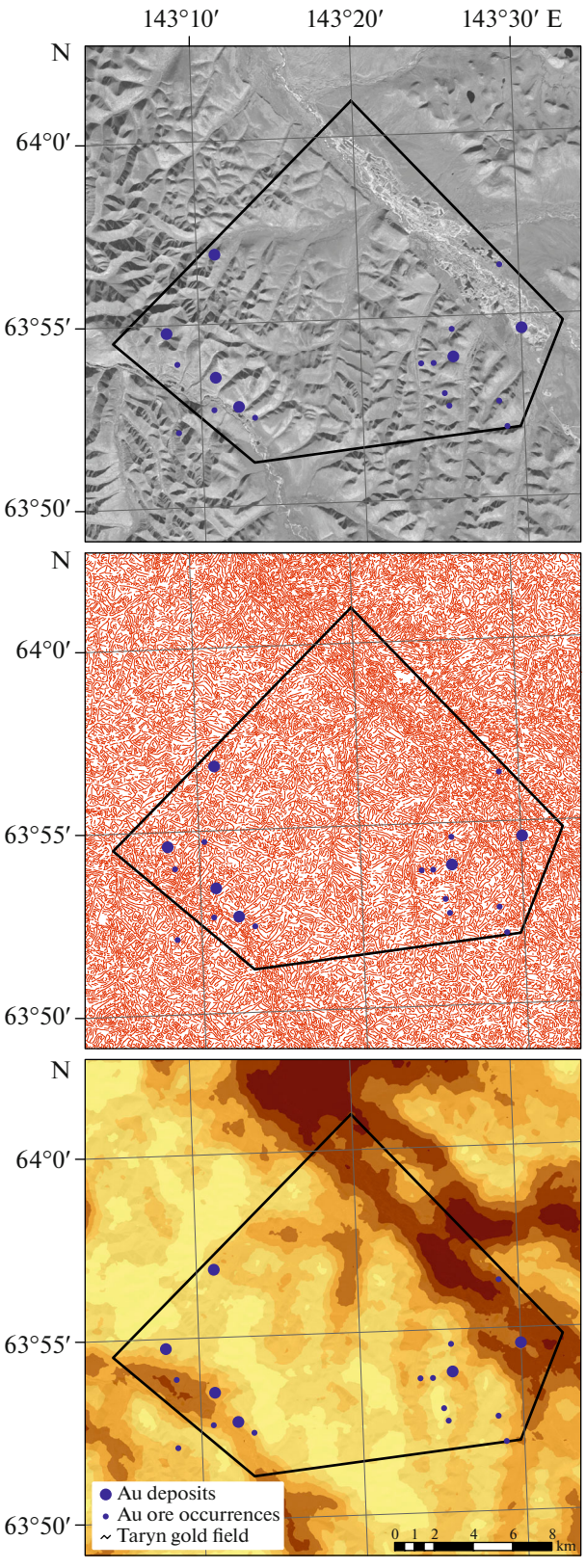

Fig. 2. Linear objects (center) highlighted in the Landsat-8 panchromatic image (top) and their specific density map (bottom).

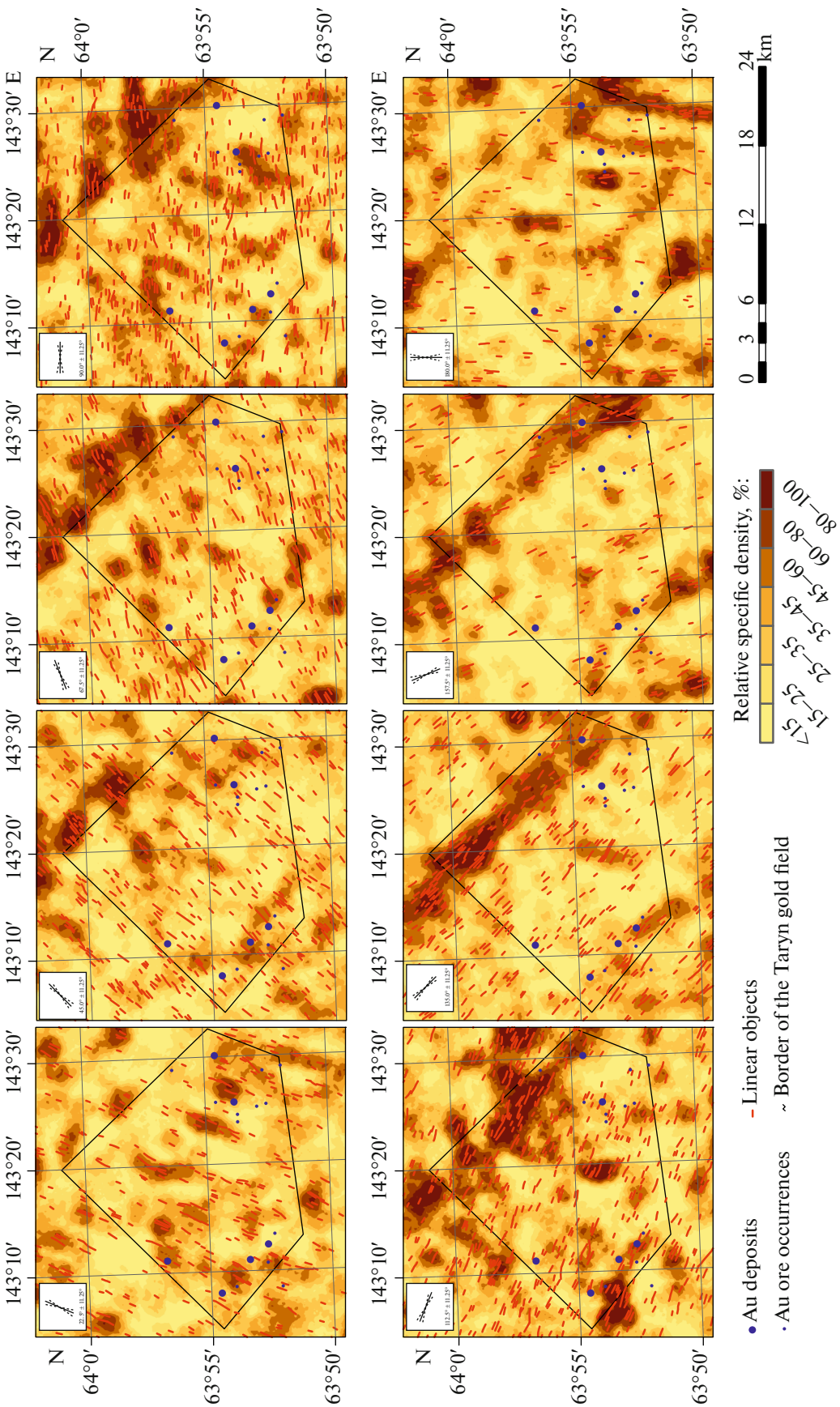

Fig. 3. Lineaments on density maps of eight different orientations (left to right, top to bottom): 22.5° ± 11.25°, 45° ± 11.25°, 67.5° ± 11.25°, 90° ± 11.25°, 112.5° ± 11.25°, 135° ± 11.25°, 157.5° ± 11.25° and 180° ± 11.25°.

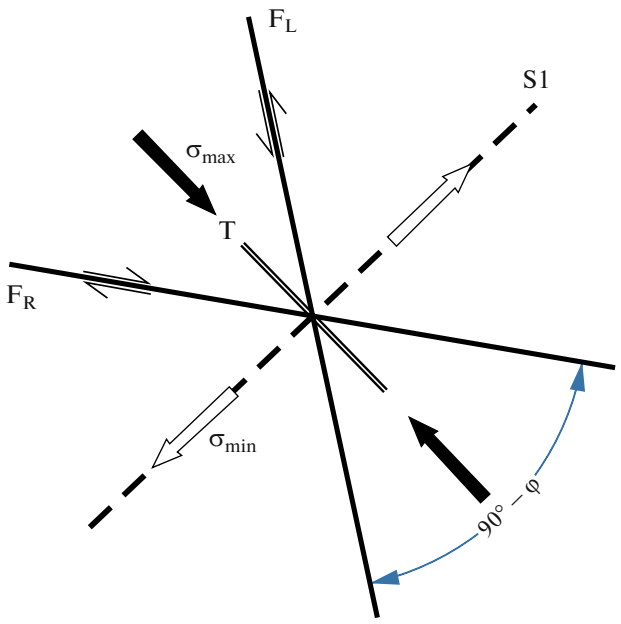

Fig. 4. Pure shear mechanism (Anderson's model).

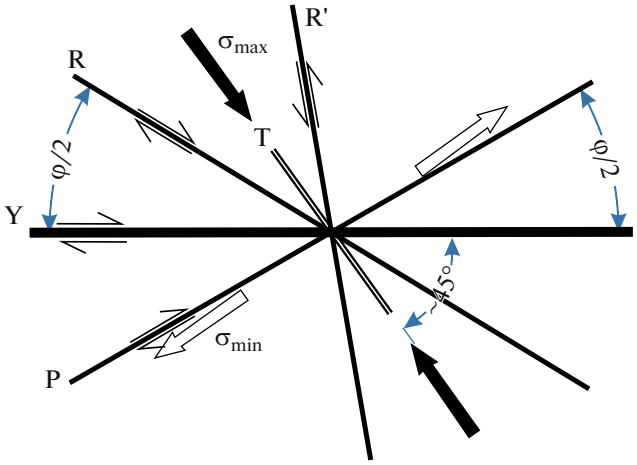

Fig. 5. Simple shear mechanism proposed by W. Riedel.

words, the relative weight of the longer segment was greater than that of a short linear object. Seven main directions of the strike of linear objects in the valley of the Bolshoi Taryn river were determined, based on the results from an analysis of our rose diagrams.

Two models were used to interpret the results:

Anderson's model (1905), a pure shear mechanism originally proposed to explain the orientation of faults in a triaxial stress field inside a homogeneous medium (Fig. 4). This mechanism assumes that the system of conjugate left–lateral F_L and right–lateral F_R fractures will form symmetrically, relative to the direction of compression at an angle between them $(90 - \varphi)°$, where φ is the angle of internal friction.

Riedel's shear model (1929) was proposed to explain the orientation of faults in a homogeneous medium

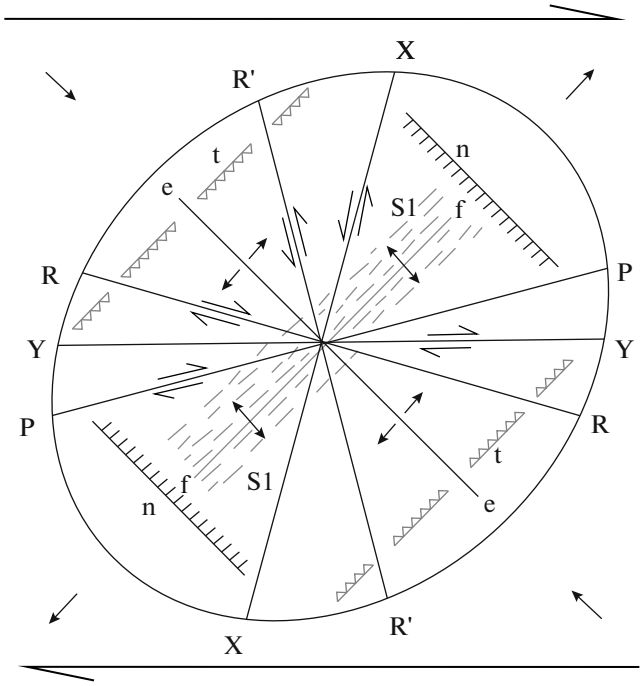

Fig. 6. Prediction of secondary structures according to Hancock (schematic diagram based on the work of P.L. Hancock) in the zone of horizontal shear localization: R and R', conjugated Riedel shears; Y, mainline shears; X, P, secondary strike–slip faults; (e) tension fractures, (n) faults, (t) reverse faults, (f) folds; S1, cleavage (Rebetskiy et al., 2017).

with a predominance of shear stresses (Fig. 5). The model assumes the formation of a series of fractures under conditions of shear stress:

- Y-shears (principle displacement zones) parallel to the direction of shearing;
- R-shears (Riedel shears) are synthetic shears with $\angle + \varphi/2$ to the direction of general shear;
- P-shears (secondary Riedel shears) are synthetic shears with $\angle - \varphi/2$ to the direction of general shear;
- R'-shears (conjugate Riedel shears) are antithetical shears with $\angle 90 - \varphi/2$ to the direction of general shear;
- T-tension fractures ($\angle \sim 45°$ to general shear) form orthogonally to the tensile stress and along the compression stress.

The most complete models of the relationship between fractures of different ranks in shearing zones can be found in other works (Hancock, 1985; Gintov, 2005; Seminskiy, 2003)

Current ideas about structures that occur in shear zones are summarized in the model shown in Fig. 6 (Rebetskiy et al., 2017).

Seven types of fractures were thus identified within the outcrop, presumably of two stages of formation (Fig. 7): synthetic (str. az. 5°–25°) and antithetical (str. az. 80°–100°); cleavage fractures (str. az. 130°–165°) and tension fractures (str. az. 30°–45°) of the first stage of formation; a stage of NE–SW compression;

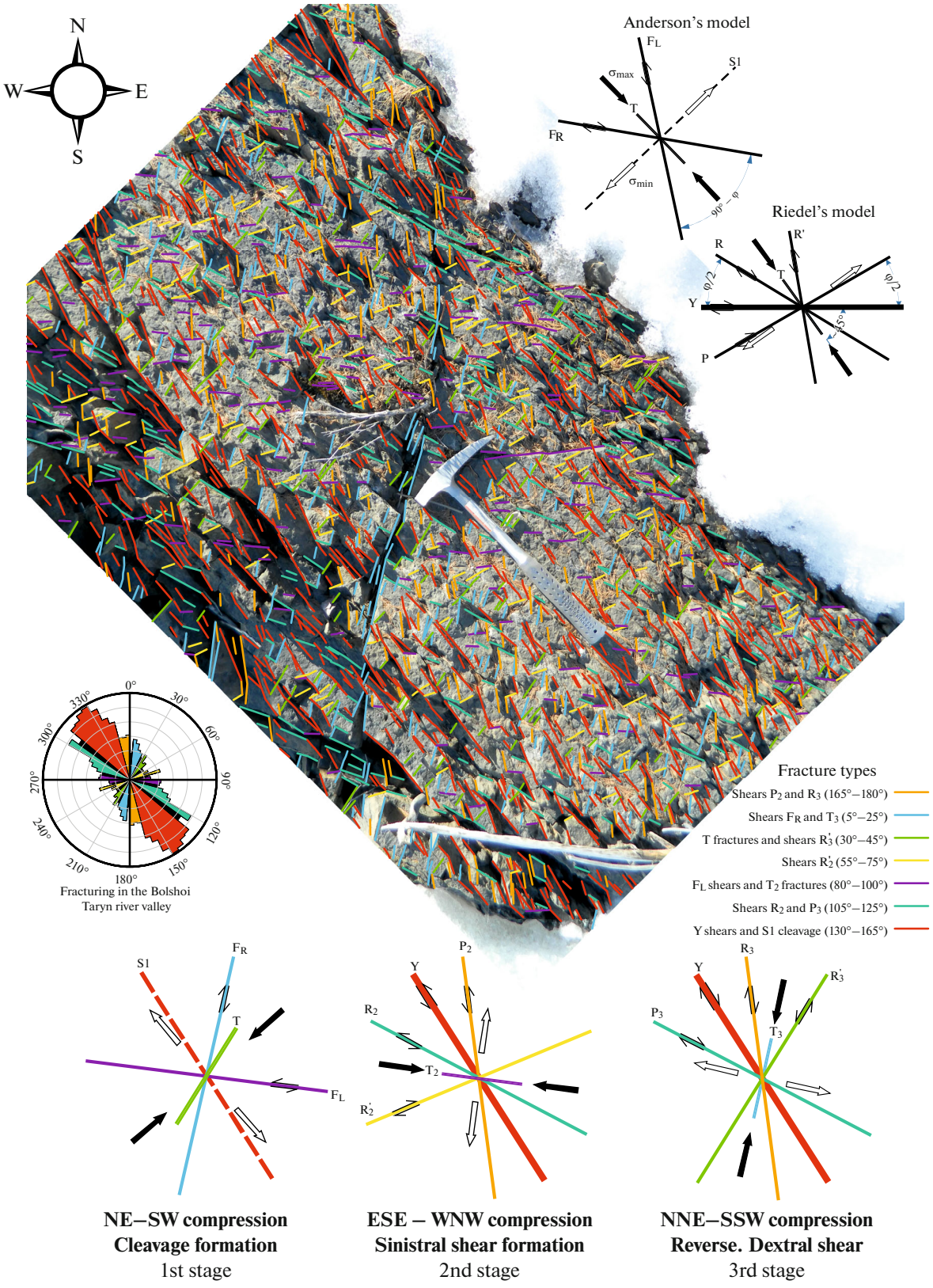

Fig. 7. Interpretation of fracture orientation in the Bolshoi Taryn river valley. Photo by A. F. Chitalin, 2016.

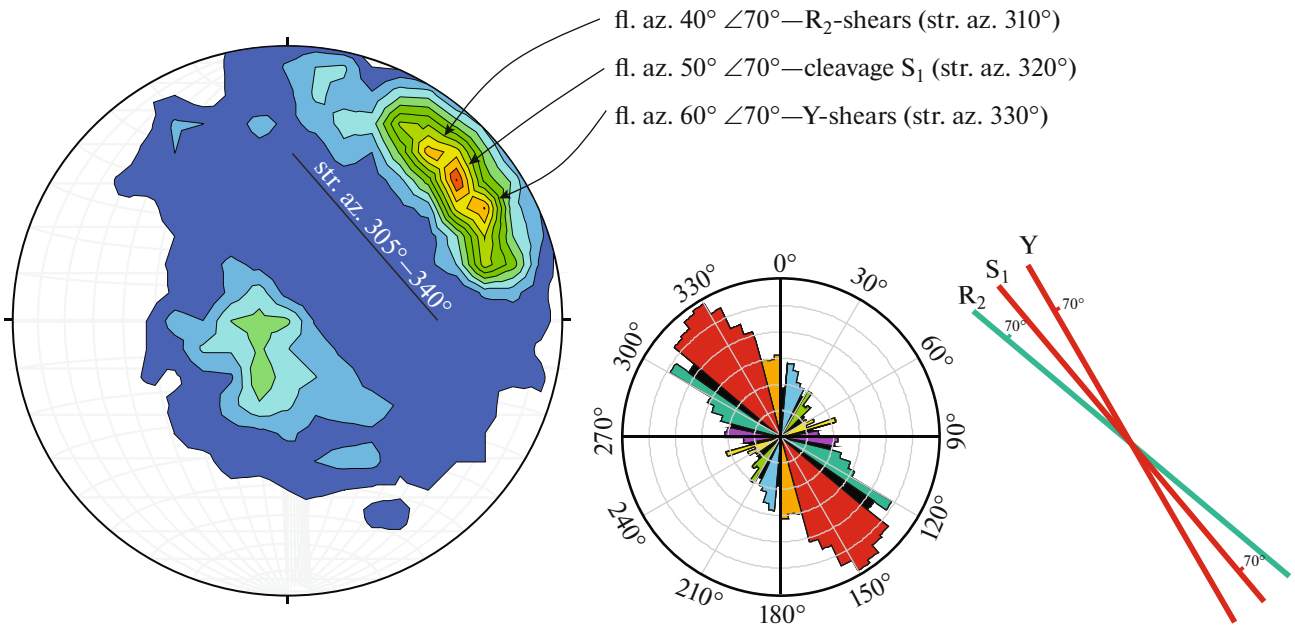

Fig. 8. Stereogram of fracturing (upper hemisphere) of the Terrasovy site.

synthetic (str. az. 105°–125° and 165°–180°), antithetical (str. az. 55°–75°) and general left-lateral strike–slip faults (str. az. 130°–165°) of the second stage; and a stage of ESE–WNW compression. At the first stage of structure formation, the axis of compression was oriented along an azimuth of 50°. Multiple cleavage fractures of the NW–SE strike formed, presumably accompanied by tension fractures perpendicular to them. In the future, the orientation of the stress axes will change to ESE–WNW (str. az. 95°), and left-side shear faults will form. These will include the Adycha–Taryn fault zone, co-directed to cleavage fractures.

STEREOGRAM ANALYSIS

Stereograms were analyzed to confirm our results, using fractures instead of lineaments as the initial data. The orientation of the fractures was determined while documenting the oriented core. The orientation of the systems, and the types of fractures and faults in both the outcrops on the daylight surface and in the core of drillholes at a depth of 200 m, are the same in the Drazhnoe gold deposit.

The drilling area closest to the outcrop is the Terrasovy site of the Drazhnoe gold deposit, where ten inclined structural drillholes have been drilled to a depth of 200 m, so data from this site was used for our confirmation. A total of 1505 measurements of fracture orientations were made within the Terrasovy site. The stereogram of fracturing for this site is shown in Fig. 8. There are four fracture density maxima on the stereogram, one of which (in the central part of the stereogram) reflects a system of sloping fractures that cannot be detected in satellite images. Three maxima are clearly visible in the upper right. These correspond to three steep-angled (∠70°) fault systems of striking fractures oriented NW–SE (str. az. 305°–340°). In analogy with the interpretation of the photo outcrop, we may assume that the system with the orientation of fl. az. 40° ∠70° corresponds to the synthetic Riedel shear of second stage of compression R_2 (the shears of this system are colored dark green in Fig. 7). The system with the orientation fl. az. 50° ∠70° most likely corresponds to the S1 cleavage fractures colored red. The third system with fl. az. 60° ∠70° presumably corresponds to the general strike–slip Y, parallel to the strike of the Adycha–Taryn zone. As in Fig. 7, the angle between strike Y and R_2 is 20°. The other systems identified in interpreting the fracturing in the valley of the Bolshoi Taryn river could correspond to maxima in the upper and lower parts of the stereograms. Because they are so weak, however, our interpretation of these maxima could be erroneous.

We performed an analysis of lineaments in the Taryn gold field similar to the one described above, based on rose diagrams of the strike for all segments (10064) of the lineaments highlighted in satellite images. Figure 10 shows a rose diagram of the strike azimuths of the segments (more than 10000) of all lineaments identified in the considered ore field. Three maxima are clearly distinguished and correspond to the strike azimuths WNW (295°), NW (315°), and N (5°). The maxima are less pronounced: 20–40, 50–60, and 80–100. If we assume the maximum of the lineaments with the strike of 310–320 corresponds to ATG lineaments and the others correspond to shear and separation structures, we can say with a high degree of confidence that the proposed orientation of the axes of compression is in this case also valid.

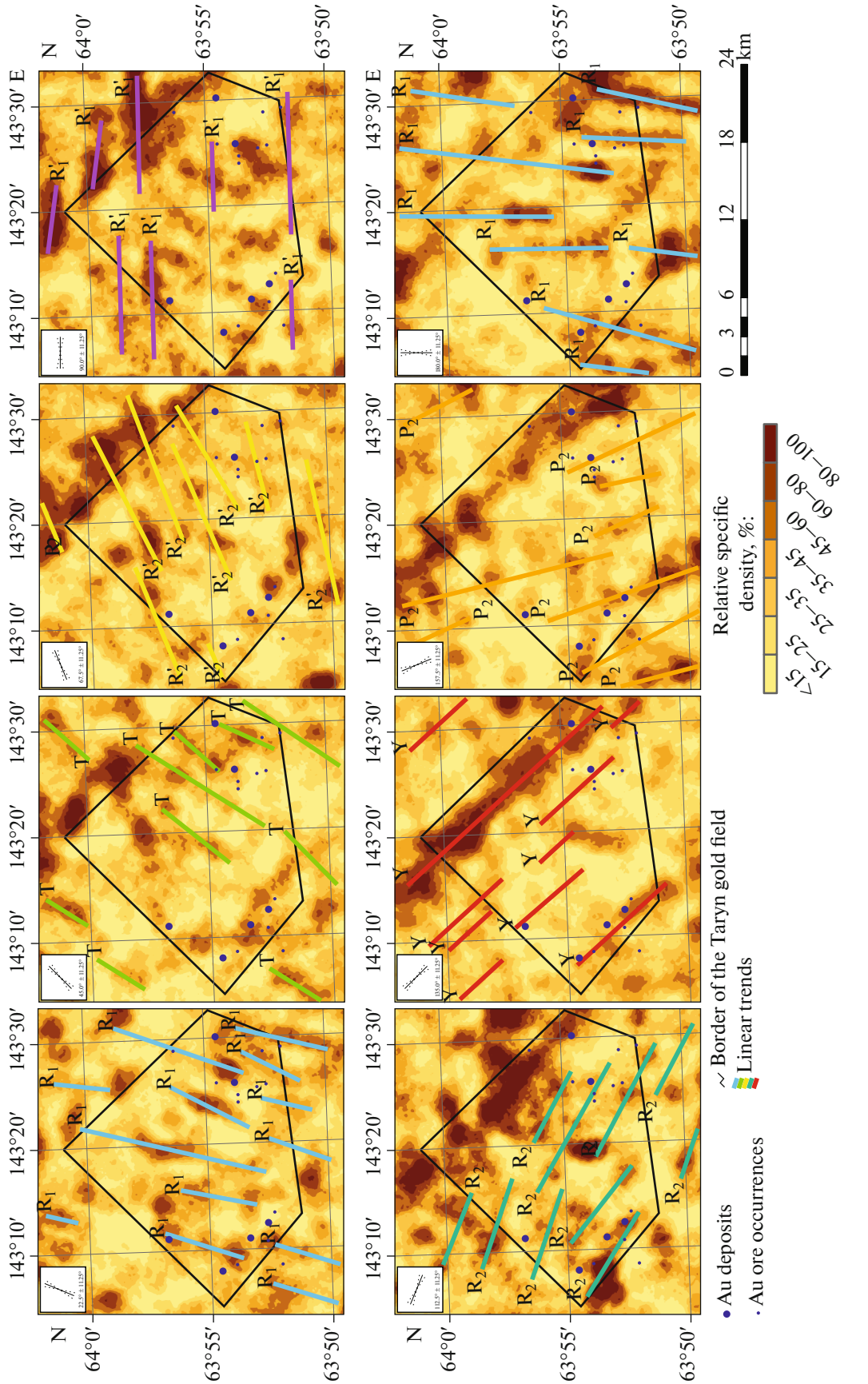

Fig. 9. Density maps of lineaments with the interpretation of trends identified in the Taryn gold field with eight different orientations (left to right, top to bottom): 22.5° ± 11.25°, 45° ± 11.25°, 67.5° ± 11.25°, 90° ± 11.25°, 112.5° ± 11.25°, 135° ± 11.25°, 157.5° ± 11.25° and 180° ± 11.25°.

Synthetic shears (Riedel shears) of the stage of NE–SW compression will thus correspond to the lineaments that form the blue maximum on the rose diagram (str. az. 0°–20°). Antithetical shears (conjugate Riedel shears) will correspond to the violet sublatitudinal maximum (str. az. 80°–100°). According to Fig. 10, cleavage S1 will correspond to the largest (red) maximum (str. az. 320°–330°), and the light green maximum (str. az. 20°–40°) will correspond to separation fractures.

Shear structures of the second stage of compression (the ESE–WNW strike) are also reflected in Fig. 10. The lineaments that form the dark green maximum on the rose diagram (str. az. 290°–310°) correspond to synthetic shears of the second stage of compression. The yellow maximum (str. az. 50°–80°) corresponds to antithetical shears (conjugate Riedel shears). According to Fig. 8, the red maximum corresponds to general shears Y (str. az. 300°–310°). The orange maximum (str. az. 340°–360°), the weakest of all, corresponds to secondary Riedel shears.

DIVISION INTO DOMAINS

To obtain representative results, statistical indicators were calculated for objects of different scales. If the moving average window was too large, the textural characteristics of small objects were obscured. If it was much smaller than the object, characteristics were determined not for the desired object, but for its smaller substructures only.

The lines of elongation of the rose diagrams allowed us to determine the orientational properties of the texture of the studied objects. This was the most stable characteristic of object orientation (Zlatopol'skiy, 2008).

Since three classes of linear objects (large, medium, and small) were identified at earlier stages of our study, rose diagrams for analyzing the spatial distribution of differently oriented stripes within the TGF were calculated using the LESSA and lines of elongation formed by a moving average window of 2000 × 2000 m (256 × 256 pixels), 1000 × 1000 m (128 × 128 pixels) and 500 × 500 m (64 × 64 pixels) (see Fig. 11).

As the size of the window grew, so did the number of stripes on whose basis of which the rose diagram was calculated, and the shape of the rose diagram was smoothed. In certain areas, such rose diagrams showed isotropy in the orientation of stripes; in others, the permanent orientation of stripes became more statistically valid (Zlatopol'skiy, 2008).

In the figure with the lines of elongation calculated using a moving average window of 256 × 256 pixels, four large domains (in the northwest, northeast, east and south) are clearly visible in addition to the linear Adycha–Taryn fault zone. Around 10 medium-sized domains can be distinguished in the similar image calculated with a window of 128 × 128 pixels, and the ATG is also clearly visible. In addition to the ATG, which stands out the most, around 20 domains can be distinguished in the most detailed image, which was calculated with a 64 × 64 pixel window.

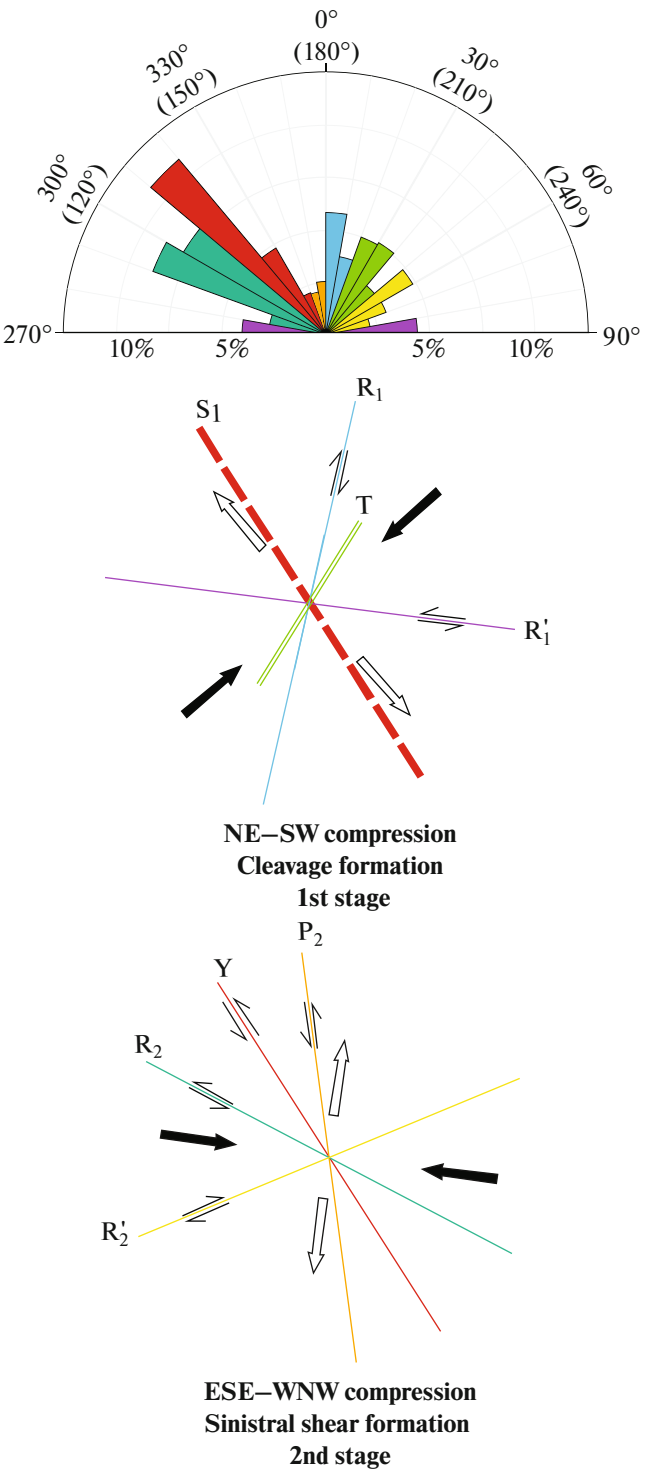

Fig. 10. Rose diagram of the strike azimuths of the lineaments (top), selected in the Taryn gold field and options for its interpretation (bottom).

Analyzing the behavior of the calculated rose diagrams and lines of elongation within the TGF, 15 domains were identified that differed in texture char-

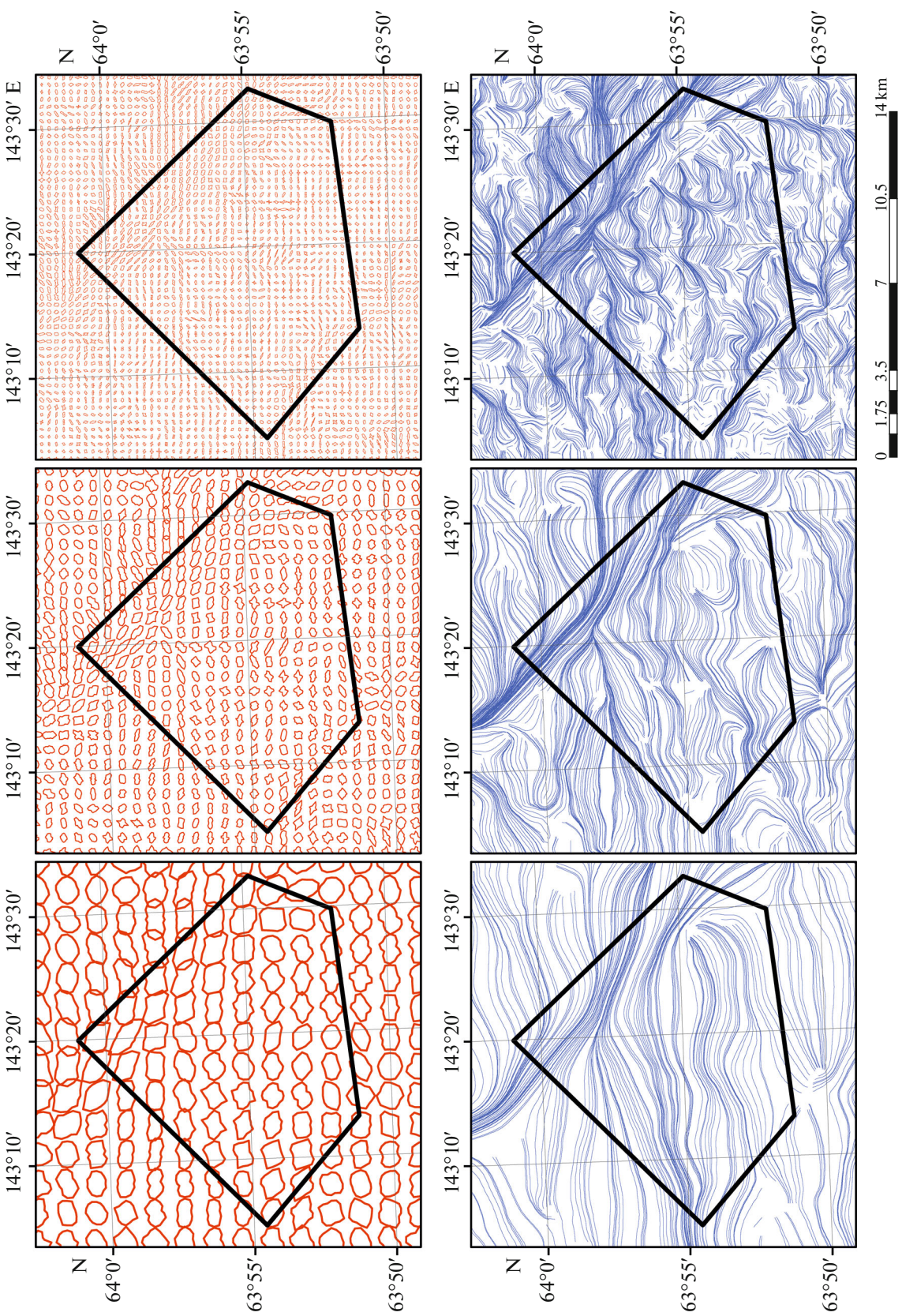

Fig. 11. Rose diagrams and lines of elongation calculated with moving average windows of 2000 × 2000 m (on left), 1000 × 1000 m (in center) and 500 × 500 m (on right).

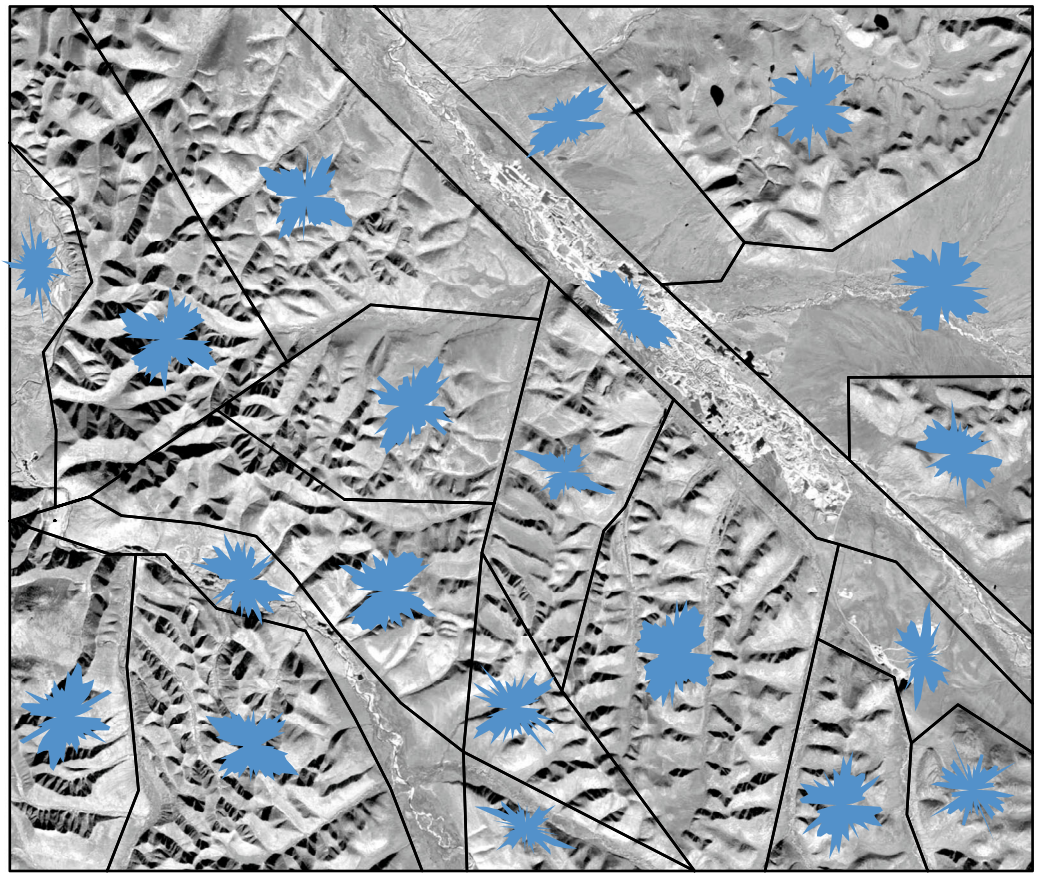

Fig. 12. Predominant orientation of stripes in the selected domains.

acteristics. Generalized rose diagrams were calculated that reflected the main characteristics of the textural features of a particular domain or a selected stripe in each domain (Fig. 12). We can see that the stripes acquire a NW–SE orientation in the valleys of the Bolshoi and Maly Taryn rivers, while the orientation of the stripes is close to chaotic in the northeastern part of the territory. In the interfluve of the Bolshoi and Maly Taryn rivers, two orthogonal directions predominate in all domains: similar to the orientation in the valleys (NW–SE) and perpendicular to it (NE–SW). This mutual arrangement of stripes could indicate a series of parallel tectonic faults in the NE and NW strikes, limited by two large strike–slip zones in the valleys of large rivers.

The predominance of NE orientation of the stripes in the central part of TGF and the lineaments of the same strike selected at earlier stages of our study testify to the established opinion about the left lateral strike–slip kinematics of the ATG. The reversible nature of the ATG is assumed, however, based on the morphology of the medium-sized lineaments adjacent to the large one in the valleys of the Bolshoi and Maly Taryn rivers (their backward bending is uncharacteristic of a sinistral shear). Left-lateral movements for disjunctive faults thus become right-lateral. Nevertheless, the orientation of the overwhelming number of stripes and lineaments in the central part of the TGF indicates the predominance of left-lateral strike–slip kinematics over right-lateral ones, even if the latter do occur.

CONCLUSIONS

Computers were used to identify several tens of thousands of differently oriented linear objects in images obtained by the Landsat-8 satellite. Calculating rose diagrams, seven systems with stable directions were identified among all multidirectional objects. In most cases, the extended lineaments corresponded to the valleys of watercourses of different orders. It was assumed that rivers and streams follow rectilinear sections of rock disintegration caused by tectonic faults coming to the surface.

The interpretation of the role of each of the systems in the formation of the TGF structure was based on two generally accepted mechanisms for the formation of tectonic faults: Anderson's model and Riedel's model. The Taryn gold field is thus located between two large zones of the thickening of NW–SE strike lineaments that correspond to regional fault zones (including the Adycha–Taryn zone) in the valley of the Bol-

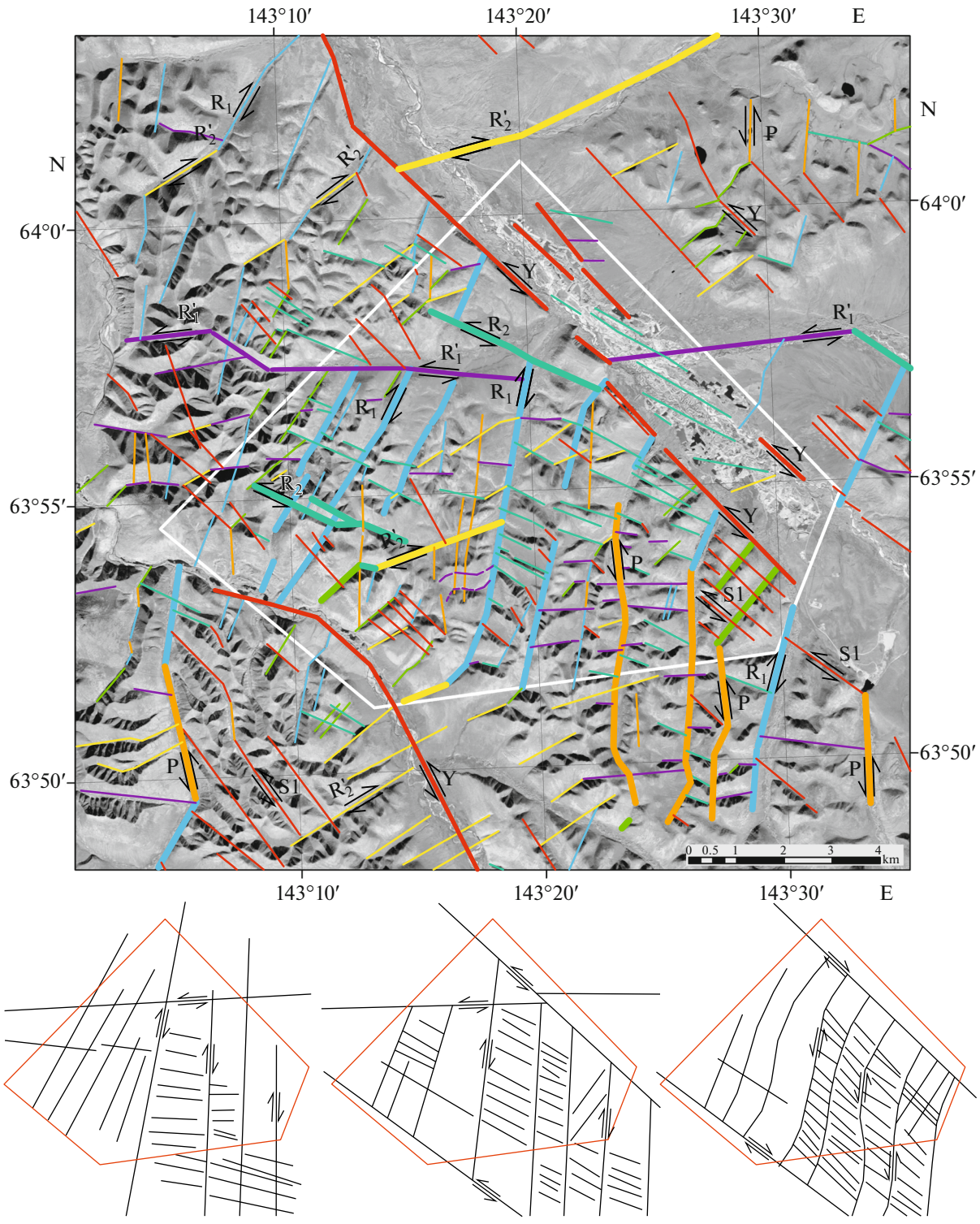

Fig. 13. Final result from interpreting the selected lineaments (top) according to the stage-by-stage formation of the modern structure of the Taryn ore field (bottom).

shoi Taryn river. It was assumed there was a series of parallel tectonic faults of the NE and NW strike in the central part of the ore field, and that these were coupled with two large strike–slip zones in the valleys of large rivers. Areas of the thickening of linear objects are clearly visible on specific density maps, standing out in the form of elongated chains of density maxima.

The orientation of the conjugated faults testifies to the predominantly left-lateral shear kinematics of the ATG. Nevertheless, the reversible nature of the ATG was assumed (i.e., the left-lateral movements became right-lateral, since uncharacteristic bending of the selected faults in the opposite direction was detected for the sinistral shear). However, the left-lateral strike–slip kinematics component obviously predominated over the right-lateral one, even if the latter did occur.

Lineaments are found throughout the TGF that probably correspond to tectonic faults of three stages of compression (Fig. 13). At the first stage, the axes of compression had a NE–SW orientation. NW–SE striking cleavage fractures, sublatitudinal left-lateral strike–slip faults, and submeridional right-lateral strike–slip faults formed. During the second stage, the axes of compression were oriented ESE–WNW. The main large left-lateral tectonic faults formed, probably following zones of cleavage faults and fractures formed at the first stage. Riedel's synthetic and antithetical shears appeared. The orientation of the axes of compression of the third stage is presumably orthogonal to the orientation of the axes in the second stage, NNE–SSW. With such mutual arrangement of the axes, the kinematics of tectonic faults reversed. Left-lateral ATG strike–slip faults became right–lateral ones, and slips occurred along the fractures of separation formed at the first stage of deformation.

A comparison of the results of lineament analysis, ones from interpreting fracturing in outcrops in the Bolshoi Taryn river valley, and data from exploratory drilling confirmed the assumed mutual position of the stress axes within the Taryn gold field. We may assume the orientation of the stress axes that existed within the Terrasovy site is also typical of the rest of the ore field.

REFERENCES

Anderson, E.M., The dynamics of faulting, *Trans. Edinburgh Geol. Soc.*, 1905, vol. 8, pp. 387–402.

Aristov, V.V., Prokofiev, V.Yu., Imamendinov, B.N., Kryazhev, S.G., Alekseev, V.Yu., and Sidorov, A.A., Ore-forming processes in the Drazhnoe gold–quartz deposit (Eastern Yakutia, Russia), *Dokl. Earth Sci.*, 2015, vol. 464, no. 1, pp. 879–884.

Berger, V.I., *Sur'myanye mestorozhdeniya* (Antimony Deposits), Moscow: Nedra, 1978.

Bondur, V.G. and Zverev, A.T., Satellite method of earthquake forecast based on the lineament analysis of system dynamics, *Issled. Zemli Kosmosa*, 2005a, no. 3, pp. 37–52.

Bondur, V.G. and Zverev, A.T., A method of earthquake forecast based on the lineament analysis of satellite images, *Dokl. Earth Sci.*, 2005b, vol. 402, no. 4, pp. 561–567.

Bondur, V.G. and Zverev, A.T., Lineament system formation mechanisms recorded in space images during the monitoring of seismic hazard areas, *Issled. Zemli Kosmosa*, 2007, no. 1, pp. 47–56.

Chitalin, A.F., Shear tectonics and gold content of the Kolyma region, *Zoloto Tekhnol.*, 2016, no. 4, pp. 122–126.

Chitalin, A.F., Voskresenskii, K.I., Grishin, E.M., Sivkov, D.V, Usenko, V.V., Fomichev, E.V., and Chikatueva, V.Yu., The structural–kinematic model the Drazhnoe gold deposit, *Geofizika*, 2018, vol. 3, pp. 106–114.

Gintov, O.B., *Polevaya tektonofizika i ee primenenie pri izuchenii deformatsii zemnoi kory Ukrainy* (Field Tectonophysics and Its Use in Studying the Earth's Core Deformation of Ukraine), Kiev: Feniks, 2005.

Hancock, P.L., Brittle microtectonics: Principles and practice, *J. Struct. Geol.*, 1985, vol. 7, nos. 3–4, pp. 437–457.

Hobbs, W.H., Lineaments of the Atlantic border region, *Geol. Soc. Am. Bull.*, 1904, vol. 15, pp. 483–506.

Indolev, L.N., Zhdanov, Yu.Ya., and Supletsov, V.M., *Sur'myanoe orudenenie Verkhoyano-Kolymskoi provintsii* (Antimony Mineralization of the Verkhoyan–Kolyma Region), Novosibirsk: Nauka, 1980.

Mokshantsev, K.B., The role of the orogenic stage in the development of platforms and layered areas on the example of the Siberian platform and the Verkhoyan–Chukotka region, in *Tektonika Sibiri* (Tectonics of Siberia), vol. 3: *Tektonika Sibirskoi platformy* (Tectonics of the Siberian Platform), Moscow: Nauka, 1970, pp. 27–40.

Parfenov, L.M., Geodynamics, magmatism, and metallogeny of the Verkhoyan–Kolyma mesozoids, in *Zakonomernosti razmeshcheniya poleznykh iskopaemykh* (Regularities of Mineral Resource Localization), Moscow, 1988, vol. 15, pp. 179–188.

Prokop'ev, A.B. and Kaskevich, G.E., Shear duplexes of East Yakutia, *Otechestvennaya Geol.*, 2000, no. 5, pp. 44–46.

Rebetskiy, Yu.L., Sim, L.A., and Marinin, A.V., *Ot zerkal skol'zheniya k tektonicheskim napryazheniyam. Metodiki i algoritmy* (From Sliding Mirrors to Tectonic Stresses), Moscow: GEOS, 2017.

Riedel, W., Zur Mechanik geologischer Brucherscheinungen, *Zentralbl. Mineral. Geol. Paleontol. B*, 1929, pp. 354–368.

Seminskiy, K.Zh., *Vnutrennyaya struktura kontinental'nykh razlomnykh zon: tektonofizicheskii aspekt* (The Internal Structure of Continental Fault Zones: The Tectonophysical Aspect), Novosibirsk: SO RAN, 2003.

Shakhtyrov, V.G., Shear structural ensembles and gold mineralization of the Yan–Kolyma fold system, *Doctoral (Geol.–Mineral.) Dissertation*, Magadan, Northeastern Integrated Scientific Research Institute, 2009.

Vladimirov, V.G., Geological structure of the Adycha–Taryn zone and regularities in the local gold–antimony mineralization, *Extended Abstract of Cand. Sci. (Geol.–Mineral.) Dissertation*, Moscow: Inst. of Mineralogy, Geochemistry, and Crystal Chemistry of Rare Elements, 1977.

Voitenko, V.N., Shear structural parageneses and gold mineralization of the Adycha–Taryn deep fault, Internet presentation, Moscow, 2015. http://www.ifz.ru/fileadmin/user_upload/subdivisions/506/OMTS/2015/26.02/Voitenko_reduce.pdf.

Zlatopol'skiy, A.A., Technique for measuring the orientation characteristics of remote sensing data (LESSA technology), *Sovrem. Probl. Distantsionnogo Zondirovaniya Zemli Kosmosa*, 2008, vol. 5, no. 1, pp. 102–112.

Translated by V. Selikhanovich